

Transmission and Reflection of Water-Wave on a Floating Ship in Vast Oceans

Amel A. Alaidrous*

Department of Mathematics, Faculty of Applied Science, Umm Al-Qura University, Makkah, Saudi Arabia

*Corresponding Author: Amel A. Alaidrous. Email: dr.amlah_gol@hotmail.com

Received: 08 November 2020; Accepted: 15 December 2020

Abstract: In this paper, we study the water-wave flow under a floating body of an incident wave in a fluid. This model simulates the phenomenon of waves abording a floating ship in a vast ocean. The same model, also simulates the phenomenon of fluid-structure interaction of a large ice sheet in waves. According to this method. We divide the region of the problem into three subregions. Solutions, satisfying the equation in the fluid mass and a part of the boundary conditions in each subregion, are given. We obtain such solutions as infinite series including unknown coefficients. We consider a limited number only of the coefficients by truncating the infinite series and satisfy the remaining boundary conditions approximately. Numerical experiments show that the results are acceptable. Tables are given along with the graph of the system of the resulting streamlines and the dynamical pressure acting on the obstacle. The drawn system of streamlines shows the correctness of the solution and the pressure is maximum on the side facing the upstream extremity of the channel. The same procedure can be adequately applied for problems with more complicated geometry and other phenomenon can thus be simulated.

Keywords: Potential flow; linear theory; fixed floating obstacle; fourier transformation; boundary collocation technique; spectral method

1 Introduction

The problem of the study of water-wave flow under an upper fixed floating obstacle is very important from theoretical and experimental points of view. This model simulates the phenomenon of waves falling on a floating ship in a vast ocean. The class including this type of problem is called the class of Cauchy–Poisson Problems (CPP).

This class of problems simulates several phenomena having geophysical interests. These models simulate the phenomenon of waves abording a floating ship in a vast ocean. The same models, also simulate the phenomenon of fluid-structure interaction of a large ice sheet in waves. We can find a discussion of this issue in [1–4]. These problems are non-linear, mixed free boundary value problems. Certain specified initial conditions may be assumed to these free boundary value problems [5,6]. Several difficulties envisage the theoretical study of these mathematical models.



This work is licensed under a Creative Commons Attribution 4.0 International License, which permits unrestricted use, distribution, and reproduction in any medium, provided the original work is properly cited.

The non-linearity of the model and the fact that the free surface is not known from the outset are some of these difficulties. Other difficulties are represented in the irregularity of the geometry of the region of the problem.

To overcome the non-linearity difficulty, the problem is treated following theories of long waves or the shallow water [7–10]. The linear theory of motion and theories of higher orders may be adopted [4,11]. Researchers usually use perturbation techniques to concur the difficulties coming from the irregularity of the region of the problem and approximate analytical solutions are sought. One may carry out the perturbation around a vertical or a horizontal line [7–9,12–16] regarding the particular geometry of the studied problem. It is impossible to obtain exact analytical solutions once the geometry deviates from being simple and other additional conditions are to be assumed on the geometry in order to obtain approximate analytical solutions. These additional conditions may include the assumption of thin barriers [7–9], or that of infinite depth [16], or mild slope and short topographies [11,13–15].

Numerical techniques are other alternatives if the analytical approach is inadequate. For a review of the numerical methods applied to CPP see [17,18] and references included. However, numerical procedures have their difficulties. These difficulties are appearing in convergence, stability, consistency, and error accumulation and need huge computations.

The spectral methods are semi-analytical methods used for the solution. Trefftz method [19,20], the procedures of perturbation [11,21], the boundary integral techniques [22,23], and the method of fundamental solutions [24] are examples of the semi-analytical methods. An original method for the study of flow over topography is given in [25]. This method is classified as a semi-analytical one.

The phenomenon of scattering of waves by an immersed or floating barrier in deep or in shallow water is a subject that attracts the attention of several authors (see for example, for analytical study [7–9], [25–34], for numerical study [29,35,36] and for experimental study [28,29,37–41]).

We follow here the method introduced by Abou-Dina et al. [25] for the study of water-wave flow under a fixed floating obstacle and for discovering the behavior of the resulting flow. Following this technique, the region of the definition of the problem is divided into three sub-regions. One of these regions contains a fixed floating body. We express the solutions satisfying the equations and conditions in the semi-infinite sub-domains with a set of unknown coefficients and elementary harmonic functions. The velocity potential function in the subdomain containing the obstacle is extended analytically through the boundary of the floating obstacle. We give a general solution in the enlarged sub-domain by applying the finite cosine Fourier transform. This solution uses another set of arbitrary constants and satisfies the system of equations and conditions on the horizontal bottom. We express the solution in the three subregions using one set only of coefficients by applying the continuity of the remaining physical quantities. This solution satisfies the system of equations and conditions of the problem except those on the fixed floating obstacle and probably on a part of the free surface. We satisfy these latter conditions and hence we get an equation in the form of a series to be fulfilled on the boundary of the obstacle and on the considered part of the free surface if necessary. The coefficients are obtained as a solution of a system of linear equations. Acceptable results obeying a certain specified error measure are given for the particular case of an obstacle with a sinusoidal boundary.

The application, dealing with this boundary of the fixed floating obstacle, ascertains the efficiency of applying this procedure for the solution. The drawn system of streamlines shows the correctness of the solution and the dynamical pressure acting on the witted surface of the fixed

floating obstacle is exhibited graphically. The pressure is found to be maximum on the side facing the incident wave and decreases till attaining its minimal values on the other side.

2 Description of the Problem

The problem is described by an infinite channel of finite depth. This channel is occupied by a fluid layer of constant density. The fluid layer is bounded from above and from below by a free surface and an impermeable horizontal bottom, respectively. A floating obstacle of arbitrary shape is partially immersed at the free surface (Fig. 1). The fixed floating barrier partially obstructs a wave propagating in the fluid. The incident wave is harmonic with frequency denoted by ω . This situation generates transmitted and reflected waves and local perturbations as well. It is required to find the coefficients of the transmission and the reflection. The local oscillations are also to be determined. The problem is studied in two dimensions. The study is carried out following the first-order theory of motion, the fluid is considered ideal and a velocity potential is assumed. We use the Cartesian frame, shown in Fig. 1. The origin of the system of coordinates is chosen in the mean horizontal line of the upper bound of the fluid, the x -axis and the y -axis are taken as shown in the figure.

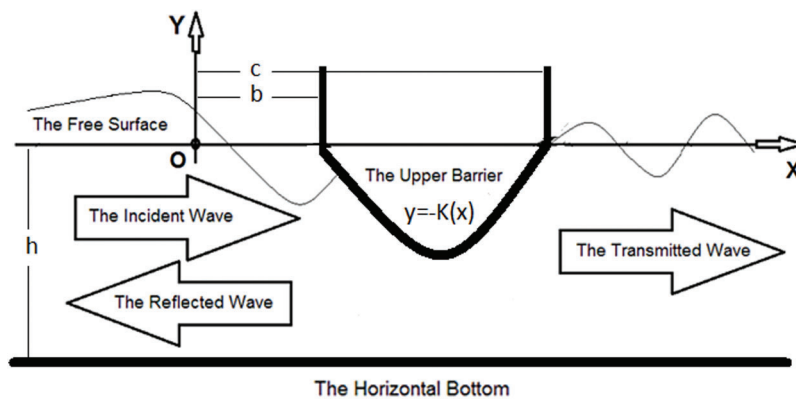


Figure 1: Description of the problem

3 System of Equations and Conditions

The horizontal line $y = 0$, $-\infty < x < b$, $c < x < \infty$ and the boundary of the immersed section of the floating obstacle $y = -K(x)$, $b \leq x \leq c$ construct higher bound of the region of the study following the linear theory. The time-independent velocity potential $\Phi(x, y)$ is defined in terms of the time-dependent one $\phi(x, y, t)$ as

$$\phi(x, y, t) = Re[\Phi(x, y) e^{-i\omega t}]. \tag{1}$$

This function satisfies the system [39]:

$$\frac{\partial^2}{\partial x^2} \Phi + \frac{\partial^2}{\partial y^2} \Phi = 0 \text{ in the region of the problem} \tag{2}$$

$$\frac{\partial}{\partial y} \Phi + \frac{\omega^2}{g} \Phi = 0, \quad (y = 0, -\infty < x < b \text{ and } c < x < \infty) \tag{3}$$

$$\frac{\partial}{\partial n}\Phi = 0, \quad (y = -K(x), b \leq x \leq c) \quad (4)$$

$$\frac{\partial}{\partial y}\Phi = 0, \quad (y = -h) \quad (5)$$

With the obvious condition that the incident wave is the only wave coming from infinity. The time-dependent functions $\eta^*(x, t)$ and $P^*(x, y, t)$, are given respectively as,

$$\eta^*(x, t) = \text{Re}[\eta(x) e^{-i\omega t}], \quad -\infty < x < b \text{ and } c < x < \infty \quad (6)$$

and

$$P^*(x, y, t) = -\rho g y + \text{Re}[P(x, y) e^{-i\omega t}]. \quad (7)$$

$\eta(x)$ and $P(x, y)$ are given as:

$$\eta(x) = \frac{i\omega}{g}\Phi(x, y) \quad \text{at } y=0, \quad -\infty < x < b \text{ and } c < x < \infty \quad (8)$$

and

$$P(x, y) = i\rho\omega\Phi(x, y) \quad (9)$$

$\Psi^*(x, y, t)$ is given as

$$\Psi^*(x, y, t) = \text{Re}[\Psi(x, y) e^{-i\omega t}] \quad (10)$$

$\Phi(x, y)$ and $\Psi(x, y)$ satisfy the relations

$$\text{grad } \Phi = -\mathbf{k} \times \text{grad } \Psi \quad (11)$$

\mathbf{k} is a unit vector parallel to the z -axis.

4 Solution

We follow the method presented by Abou-Dina et al. [6] to get a solution for the above system of equations and conditions.

The region bounded by $x = 0$ and $x = a$ contains the floating barrier. The region of the problem is thus divided into three subregions: V^- , V^0 , and V^+ as shown in (Fig. 2).

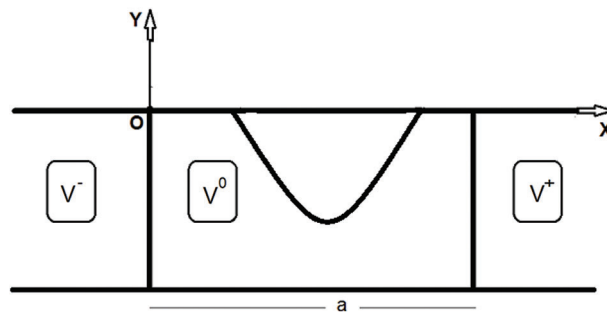


Figure 2: The three subregions V^- , V^0 , and V^+

We will solve the problem and the solution includes certain unknown coefficients. The equation in the fluid mass and a part of the boundary conditions are satisfied by this solution. Applying the continuity of the physical quantities at $x = 0$ and $x = a$ will relate the solutions in the neighboring subregions. We determine the unknown coefficients approximately.

4.1 Study in the Semi-Infinite Domains

Applying the method of separation of variables for the solution of the system of equations and conditions in the regions V^- and V^+ the solution is obtained in these semi-infinite regions respectively as [5,6]

$$\Phi^-(x, y) = \{I_0 e^{i\lambda_0 x} + R_0 e^{-i\lambda_0 x}\} \cosh \lambda_0 (y + h) + \sum_{p=1}^{\infty} R_p \cos \lambda_p (y + h) e^{\lambda_p x} \quad (12)$$

and

$$\Phi^+(x, y) = T_0 \cosh \lambda_0 (y + h) e^{i\lambda_0 (x-a)} + \sum_{p=1}^{\infty} T_p \cos \lambda_p (y + h) e^{-\lambda_p (x-a)} \quad (13)$$

where $\lambda_0 > 0$ denotes the root of the equation

$$\lambda \tanh \lambda h = \frac{\omega^2}{g} \quad (14)$$

and $\lambda_p > 0$ ($p = 1, 2, 3, \dots$) denote the roots of the equation

$$\lambda \tanh \lambda h = \frac{\omega^2}{g} \quad (15)$$

I_0 , R_0 , and T_0 are the amplitudes of the incident, the reflected and the transmitted waves respectively. R_p and T_p are complex constant coefficients. The obtained solution includes progressive waves going towards the channel extremities and local perturbations decaying in going away from the obstacle. It is required to calculate the coefficients R_0 , T_0 , R_p and T_p .

4.2 Solution in the Area V^0

$\Phi^0(x, y)$ is the potential in the area V^0 . This function satisfies Laplace's equation in V^0 and is continuous on $\overline{V^0}$. The function $\Psi^0(x, y)$ is constant on the boundary of the floating barrier. Therefore, the function $\Phi^0(x, y)$ can be extended on the area $OABC$ of Fig. 3. The extended function is harmonic on the extended region and is denoted by V . If the domain of the problem is multi connected, i.e., it contains holes then this holes are removed and replaced by suitable sources (logarithmic sources) and this has been studied in [27]. Also if there is an external pressure acting on the free surface [22] or a finite part the bottom of the channel is set in motion, the same procedure is applied but the control region V is enlarged to include the parts of the external pressure or the moving bottom.

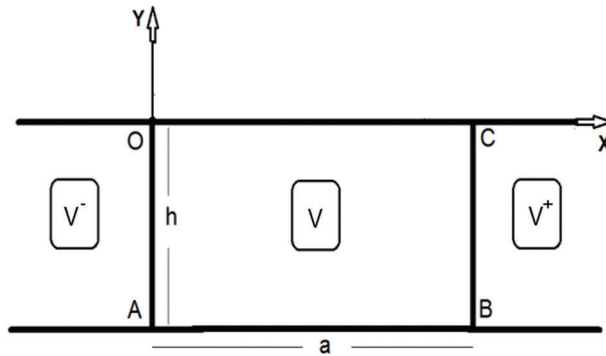


Figure 3: The extended domain

The extended function will also be denoted by $\Phi^0(x, y)$. The system of equations and conditions satisfied by function $\Phi^0(x, y)$ is given as:

$$\frac{\partial^2}{\partial x^2} \Phi^0 + \frac{\partial^2}{\partial y^2} \Phi^0 = 0, \quad 0 \leq x \leq a, \quad -h \leq y \leq 0. \quad (16)$$

$$\Phi^0(0, y) = \{I_0 + R_0\} \cosh \lambda_0 (y + h) + \sum_{p=1}^{\infty} R_p \cos \lambda_p (y + h), \quad x = 0, \quad -h \leq y \leq 0 \quad (17)$$

$$\frac{\partial \Phi^0}{\partial x}(0, y) = i \lambda_0 \{I_0 - R_0\} \cosh \lambda_0 (y + h) + \sum_{p=1}^{\infty} R_p \cos \lambda_p (y + h), \quad x = 0, \quad -h \leq y \leq 0 \quad (18)$$

$$\Phi^0(a, y) = T_0 \cosh \lambda_0 (y + h) + \sum_{p=1}^{\infty} T_p \cos \lambda_p (y + h), \quad x = a, \quad -h \leq y \leq 0 \quad (19)$$

$$\frac{\partial \Phi^0}{\partial x}(a, y) = i \lambda_0 T_0 \cosh \lambda_0 (y + h) - \sum_{p=1}^{\infty} \lambda_p T_p \cos \lambda_p (y + h), \quad x = a, \quad -h \leq y \leq 0 \quad (20)$$

and

$$\frac{\partial \Phi^0}{\partial y}(x, y) = 0, \quad 0 \leq x \leq a, \quad y = -h. \quad (21)$$

We use the transform $\widetilde{\Phi}_m^0(y)$ of $\Phi^0(x, y)$ defined as [42]:

$$\widetilde{\Phi}_m^0(y) = \int_0^{+a} \Phi^0(x, y) \cos\left(m \frac{\pi}{a} x\right) dx, \quad m = 0, 1, 2, 3, \dots \quad (22)$$

Applying this transformation to Eqs. (16), (18) and (20)–(22), the functions $\widetilde{\Phi}_m^0(y)$, $m = 0, 1, 2, 3, \dots$ are obtained after some manipulation in terms of constant coefficients a_m as

$$\begin{aligned} \widetilde{\Phi}_m^0(y) &= \frac{aI_0}{2 - \delta_m^0} \left[a_m \cosh \frac{m\pi}{a} (y+h) \right] - i[(R_0 - I_0) + (-1)^m T_0] \frac{\lambda_0}{\lambda_0^2 - (m\frac{\pi}{a})^2} \cosh \lambda_0 (y+h) \\ &\quad - \sum_{p=1}^{\infty} [R_p + (-1)^m T_p] \frac{\lambda_p}{\lambda_p^2 - (m\frac{\pi}{a})^2} \cos \lambda_p (y+h) \end{aligned} \tag{23}$$

The finite Fourier transform (23) has the following inversion expression [42]:

$$\Phi^0(x, y) = \sum_{m=0}^{\infty} \frac{2 - \delta_m^0}{a} \widetilde{\Phi}_m^0(y) \cos \left(m\frac{\pi}{a}x \right) \tag{24}$$

Using (23) and (24) together with the expressions

$$\sum_{m=0}^{\infty} \frac{(2 - \delta_m^0)}{a} \frac{(-1)^m \lambda_0}{\lambda_0^2 - (m\frac{\pi}{a})^2} \cos \left(\frac{m\pi}{a}x \right) = \frac{1}{\sin(\lambda_0 a)} \cos(\lambda_0 x) \tag{25}$$

and

$$\sum_{m=0}^{\infty} \frac{(2 - \delta_m^0)}{a} \frac{(-1)^m \lambda_p}{\lambda_p^2 - (m\frac{\pi}{a})^2} \cos \left(\frac{m\pi}{a}x \right) = \frac{1}{\sinh(\lambda_p a)} \cosh(\lambda_p x), \tag{26}$$

the velocity potential in the domain V^0 is obtained as

$$\begin{aligned} \Phi^0(x, y) &= I_0 \sum_{m=0}^{\infty} a_m \cosh \frac{m\pi}{a} (y+h) \cos \left(m\frac{\pi}{a}x \right) - i[(R_0 - I_0) \cos \lambda_0 (x-a) \\ &\quad + T_0 \cos \lambda_0 x] \frac{\cosh \lambda_0 (y+h)}{\sin(\lambda_0 a)} - \sum_{p=1}^{\infty} [R_p \cosh \lambda_p (x-a) + T_p \cosh(\lambda_p x)] \frac{\cos \lambda_p (y+h)}{\sinh(\lambda_p a)} \end{aligned} \tag{27}$$

Substituting expression (27) of $\Phi^0(x, y)$ into conditions (17) and (19), we get the following relations

$$\begin{aligned} &\{I_0 + R_0\} \cosh \lambda_0 (y+h) + \sum_{p=1}^{\infty} R_p \cos \lambda_p (y+h) \\ &= I_0 \sum_{m=0}^{\infty} a_m \cosh \frac{m\pi}{a} (y+h) - i[(R_0 - I_0) \cos \lambda_0 a + T_0] \frac{\cosh \lambda_0 (y+h)}{\sin(\lambda_0 a)} \\ &\quad - \sum_{p=1}^{\infty} [R_p \cosh \lambda_p a + T_p] \frac{\cos \lambda_p (y+h)}{\sinh(\lambda_p a)} \end{aligned} \tag{28}$$

and

$$\begin{aligned}
 & T_0 \cosh \lambda_0 (y+h) + \sum_{p=1}^{\infty} T_p \cos \lambda_p (y+h) \\
 &= I_0 \sum_{m=0}^{\infty} (-1)^m a_m \cosh \frac{m\pi}{a} (y+h) - i[(R_0 - I_0) + T_0 \cos \lambda_0 a] \frac{\cosh \lambda_0 (y+h)}{\sin (\lambda_0 a)} \\
 &\quad - \sum_{p=1}^{\infty} [R_p + T_p \cosh (\lambda_p a)] \frac{\cos \lambda_p (y+h)}{\sinh (\lambda_p a)}. \tag{29}
 \end{aligned}$$

The orthogonality of the functions $\{\cosh \lambda_0 (y+h), \cos \lambda_p (y+h), p \geq 1\}$, over $-h \leq y \leq 0$, is used. The coefficients R_0, T_0, R_p and $T_p, p \geq 1$ are obtained by the use of relations (28) and (29), in the form:

$$R_0 = I_0 \sum_{m=0}^{\infty} \{1 - (-1)^m e^{i\lambda_0 a}\} \alpha_{0,m} a_m, \tag{30}$$

$$T_0 = I_0 \left[e^{i\lambda_0 a} + \sum_{m=0}^{\infty} \{(-1)^m - e^{i\lambda_0 a}\} \alpha_{0,m} a_m, \right] \tag{31}$$

$$R_p = I_0 \sum_{m=0}^{\infty} \{1 - (-1)^m e^{-\lambda_p a}\} \alpha_{p,m} a_m, \tag{32}$$

and

$$T_p = I_0 \sum_{m=0}^{\infty} \{(-1)^m - e^{-\lambda_p a}\} \alpha_{p,m} a_m, \tag{33}$$

where $\alpha_{0,m}$ and $\alpha_{p,m}$ are given for $p \geq 1$. and $m \geq 0$. as

$$\alpha_{0,m} = \frac{\lambda_0 \cosh (\lambda_0 h) \left[\frac{m\pi}{a} \sinh \left(\frac{m\pi}{a} h \right) - \frac{\omega^2}{g} \cosh \left(\frac{m\pi}{a} h \right) \right]}{\left[\left(\frac{m\pi}{a} \right)^2 - \lambda_0^2 \right] [\lambda_0 h + \sinh (\lambda_0 h) \cosh (\lambda_0 h)]} \tag{34}$$

and

$$\alpha_{p,m} = \frac{\lambda_p \cos (\lambda_p h) \left[\frac{m\pi}{a} \sinh \left(\frac{m\pi}{a} h \right) - \frac{\omega^2}{g} \cosh \left(\frac{m\pi}{a} h \right) \right]}{\left[\lambda_p^2 + \left(\frac{m\pi}{a} \right)^2 \right] [\lambda_p h + \sin (\lambda_p h) \cos (\lambda_p h)]}. \tag{35}$$

The function $\Phi^0(x, y)$ given by (27) is written using (30)–(33) in terms of $a_m, m \geq 0$ as

$$\Phi^0(x, y) = I_0 \left[e^{i\lambda_0 x} \cosh \lambda_0 (y+h) + \sum_{m=0}^{\infty} a_m \Phi_m^0(x, y) \right] \tag{36}$$

where $\Phi_m^0(x, y)$, $m \geq 0$ are given as:

$$\begin{aligned} \Phi_m^0(x, y) = & \cosh \frac{m\pi}{a}(y+h) \cos\left(\frac{m\pi}{a}x\right) - \alpha_{0,m} \left(e^{i\lambda_0 x} + (-1)^m e^{i\lambda_0(x-a)} \right) \cosh \lambda_0(y+h) \\ & - \sum_{p=1}^{\infty} \alpha_{p,m} \left(e^{-\lambda_p x} + (-1)^m e^{-\lambda_p(x-a)} \right) \cos \lambda_p(y+h). \end{aligned} \tag{37}$$

The functions $\Psi^-(x, y)$, $\Psi^0(x, y)$ and $\Psi^+(x, y)$ are obtained from relations (11), (14), (15), (36) and (37) as

$$\Psi^-(x, y) = i \{ I_0 e^{i\lambda_0 x} - R_0 e^{-i\lambda_0 x} \} \sinh \lambda_0(y+h) + \sum_{p=1}^{\infty} R_p \sin \lambda_p(y+h) e^{\lambda_p x}, \tag{38}$$

$$\Psi^0(x, y) = I_0 \left[e^{i\lambda_0 x} \sinh \lambda_0(y+h) - \sum_{m=0}^{\infty} a_m \Psi_m^0(x, y) \right], \tag{39}$$

and

$$\Psi^+(x, y) = iT_0 \sinh \lambda_0(y+h) e^{i\lambda_0(x-a)} - \sum_{p=1}^{\infty} T_p \sin \lambda_p(y+h) e^{-\lambda_p(x-a)}, \tag{40}$$

The functions $\Psi_m^0(x, y)$, $m = 1, 2, 3, \dots$ are defined as

$$\begin{aligned} \Phi_m^0(x, y) = & \sinh \frac{m\pi}{a}(y+h) \sin\left(\frac{m\pi}{a}x\right) + i\alpha_{0,m} \left(e^{i\lambda_0 x} - (-1)^m e^{-i\lambda_0(x-a)} \right) \sinh \lambda_0(y+h) \\ & - \sum_{p=1}^{\infty} \alpha_{p,m} \left(e^{-\lambda_p x} - (-1)^m e^{\lambda_p(x-a)} \right) \sin \lambda_p(y+h). \end{aligned} \tag{41}$$

It can be shown using expressions (14) and (15) together with the boundary conditions on the upper and lower bounds of the control region V^0 that

$$|T_0|^2 + |R_0|^2 = |I_0|^2 \tag{42}$$

Eq. (42) translates the conservation of energy. The conservation of mass is satisfied if

$$T_0 + R_0 = I_0 \tag{43}$$

which becomes an identity, if we set

$$a = 2k\pi/\lambda_0, \tag{44}$$

where $k > 0$ is an integer. $k > 0$ is taken as the smallest integer (k_0) making the sub-domain V^0 enclose the fixed floating obstacle.

4.3 The Approximate Solution

To get the functions $\Phi(x, y)$ and $\Psi(x, y)$, in the whole region of the problem, in terms of a_m , $m \geq 0$, we collect relations (14), (15) and (36) for $\Phi(x, y)$ and (38)–(40) for $\Psi(x, y)$. These functions satisfy the equations of the problem except the condition on the higher bound of V^0 (see Fig. 2). We satisfy this condition approximately to determine a_m , $m = 0, 1, 2, 3, \dots$

As shown in Fig. 2, the upper bound of the sub-domain V^0 consists of two parts of the free surface lying on both sides of the floating obstacle, precisely at $0 \leq x < b$ and $c < x \leq a$, in addition to a third part represented by the lower boundary of the obstacle with equation $y = -K(x)$, $b \leq x \leq c$. In the frame of the linear theory of motion adopted here, the condition on the free surface, at $0 \leq x < b$ and $c < x \leq a$, reduces to

$$\frac{\partial}{\partial y} \Phi^0(x, y) - \frac{\omega^2}{g} \Phi^0(x, y) = 0 \quad \text{at } y = 0, \quad 0 \leq x < b \text{ and } c < x \leq a, \quad (45)$$

which together with expression (36) lead to the following constraints posed on a_m , $m = 0, 1, 2, 3, \dots$

$$\frac{\partial}{\partial y} \left[e^{i\lambda_0 x} \cosh \lambda_0 (y+h) + \sum_{m=0}^{\infty} a_m \Phi_m^0(x, y) \right] - \frac{\omega^2}{g} \left[e^{i\lambda_0 x} \cosh \lambda_0 (y+h) + \sum_{m=0}^{\infty} a_m \Phi_m^0(x, y) \right] = 0, \quad (46)$$

at $y = 0$, $0 \leq x < b$ and $c < x \leq a$,

$\Phi_m^0(x, y)$ are defined by (37). Relations (46) are simplified as

$$\sum_{m=0}^{\infty} a_m \left[\frac{m\pi}{a} \sinh \left(\frac{m\pi}{a} h \right) - \frac{\omega^2}{g} \cosh \left(\frac{m\pi}{a} h \right) \right] \cos \left(\frac{m\pi}{a} x \right) = 0, \quad 0 \leq x < b \text{ and } c < x \leq a, \quad (47)$$

On the other hand, the function $\Psi(x, y)$, given by (43)–(45), should have a constant value on the boundary of the floating obstacle ($y = -K(x)$, $b \leq x \leq c$) since this boundary is a part of a certain streamline. Therefore, the coefficients a_m has also to obey the following series equation

$$\sum_{m=0}^{\infty} a_m \Psi_m^0(x, y) = \frac{C_0}{I_0} + i e^{i\lambda_0 x} \sinh \lambda_0 (y+h), \quad y = -K(x), \quad b \leq x \leq c, \quad (48)$$

where C_0 denotes the constant value taken by the stream-function $\Psi(x, y)$ on the barrier with equation $y = -K(x)$, $b \leq x \leq c$ (see Fig. 1 for the constants b, c). Let x_0 be a point arbitrarily chosen in the interval $b \leq x \leq c$ with $y_0 = -K(x_0)$. Condition (48) may be replaced by the following

$$\sum_{m=0}^{\infty} a_m \left[\Psi_m^0(x, y) - \Psi_m^0(x_0, y_0) \right] = i \left[e^{i\lambda_0 x} \sinh \lambda_0 (y+h) - e^{i\lambda_0 x_0} \sinh \lambda_0 (y_0+h) \right], \quad y = -K(x), \quad (49)$$

$b \leq x \leq c,$

If the floating obstacle occupies the interval $0 \leq x \leq a$, and no part of the free surface is enclosed in this interval then expression (49) only is to be considered and expressions (47) are discarded. We hence give the solution to the problem in terms of a set of coefficients a_m . To determine the coefficients of expressions (47, 49), we follow the collocation procedure [39,40]. We replace the infinite upper limit of the series on the L.H.S. of both expressions (47) and (49)

by M has taken sufficiently large according to the desired accuracy. We choose a decomposition $\{x_n, n = 0, 1, 2, \dots, N_1, \dots, N_2, \dots, N\}$ for $0 \leq x \leq a$ such that $0 = x_0 < x_1 < \dots < x_{N_1} = b < \dots < x_{N_2} = c < \dots < x_N = a$, where N is an integer with $N > M$. We thus obtain the following system of equations

$$\sum_{m=0}^{\infty} B_{m,n} a_m^{(N,M)} = D_n, \quad n = 1, 2, \dots, N, \tag{50}$$

The elements $B_{m,n}$ and D_n are

$$\left. \begin{aligned} B_{m,n} &= \left[\frac{m\pi}{a} \sinh\left(\frac{m\pi}{a}h\right) - \frac{\omega^2}{g} \cosh\left(\frac{m\pi}{a}h\right) \right] \cos\left(\frac{m\pi}{a}x_n\right), \\ D_n &= 0 \quad \text{for } n = 0, 1, 2, \dots, N_1 \text{ and } m = 1, 2, \dots, M, \end{aligned} \right\} \tag{51}$$

and

$$B_{m,n} = \Psi_m^0(x_n - K(x_n)), D_n = ie^{i\lambda_0 x_n} \sinh(h - K(x_n)) \quad \text{for } n = N_1 + 1, \dots, N_2 - 1 \text{ and } m = 1, 2, \dots, M. \tag{52}$$

We have a number N of linear Eqs. (50)–(52) in a number M of the coefficients $a_m^{(N,M)}$ with $N > M$. We put this system in the following square form

$$(\mathbf{B}^T \mathbf{B}) \mathbf{A} = \mathbf{B}^T \mathbf{D} \tag{53}$$

where \mathbf{A} is the vector of unknown coefficients $a_m^{(N,M)}$, \mathbf{B}^T is the transpose of the matrix \mathbf{B} and \mathbf{D} is the vector of constants D_n . The solution of the system (53) determines the velocity potential $\Phi^0(x, y)$ and the stream-function $\Psi^0(x, y)$, in the sub-region V^0 as

$$\Phi^{0(N,M)}(x, y) = I_0 \left[e^{i\lambda_0 x} \cosh \lambda_0 (y + h) + \sum_{m=0}^M a_m^{(N,M)} \Phi_m^0(x, y) \right], \tag{54}$$

and

$$\Psi^{0(N,M)}(x, y) = I_0 \left[e^{i\lambda_0 x} \sinh \lambda_0 (y + h) - \sum_{m=0}^M a_m^{(N,M)} \Psi_m^0(x, y) \right], \tag{55}$$

respectively.

The function $\Phi^{0(N,M)}(x, y)$ given by (54) satisfies approximately a relation of the form (45) and the function $\Psi^{0(N,M)}(x, y)$ given by (55) has approximately a constant value along the

boundary of the immersed part of the obstacle. We introduce $ER^{(N,M)}(x)$, $0 \leq x \leq a$, as local error with:

$$ER^{(N,M)}(x) = \begin{cases} \sum_{m=0}^M a_m^{(N,M)} \left[\frac{m\pi}{a} \sinh\left(\frac{m\pi}{a}h\right) - \frac{\omega^2}{g} \cosh\left(\frac{m\pi}{a}h\right) \right] \cos\left(\frac{m\pi}{a}x\right), \\ \text{for } 0 \leq x < b, \quad c < x \leq a \\ \sum_{m=0}^M a_m^{(N,M)} [\Psi_m^0(x, y) - \Psi_m^0(x_0, y_0)], \\ -i[e^{i\lambda_0 x} \sinh \lambda_0 (y + h) - e^{i\lambda_0 x_0} \sinh \lambda_0 (y_0 + h)], \\ \text{for } y = -K(x), \quad b \leq x \leq c \end{cases} \tag{56}$$

By checking the inequality

$$ER_L^{(N,M)} = \max_{0 \leq x \leq a} |ER^{(N,M)}(x)| < \varepsilon \tag{57}$$

for a control parameter ε , the choice of N and M can be controlled. Also, this can be done by checking another inequality of the form

$$ER_G^{(N,M)} = \frac{1}{a} \int_0^a |ER^{(N,M)}(x)| dx < \varepsilon \tag{58}$$

We start with a choice of N and M , then if (4.46) (or (4.47)) is not satisfied, the values of N and M are increased, and we restart the technique to obtaining the desired result. The straight forward collocation technique is met by setting $N = M + 1$.

Approximate expressions for R_0 and T_0 are then given as

$$R_0^{(N,M)} = I_0 \sum_{m=0}^M \{1 - (-1)^m e^{i\lambda_0 a}\} \alpha_{0,m} a_m^{(N,M)}, \tag{59}$$

and

$$T_0^{(N,M)} = I_0 \left[e^{i\lambda_0 a} + \sum_{m=0}^M \{(-1)^m - e^{i\lambda_0 a}\} \alpha_{0,m} a_m^{(N,M)}, \right] \tag{60}$$

respectively.

5 Numerical Experiments for a Floating Obstacle of a Sinusoidal Boundary

As a numerical experiment, we consider the case of a fixed floating obstacle with a lower immersed part of a sinusoidal boundary with H as a maximum depth and width W . $K(x)$ is considered as

$$K(x) = \frac{H}{2} \left[1 - \cos\left(\frac{2\pi(x-b)}{c-b}\right) \right] \quad \text{for } b \leq x \leq c. \tag{61}$$

The constant k_0 is chosen such that $a = \frac{2k_0\pi}{\lambda_0}$. k_0 is the smallest integer satisfying this relation in such a way that the finite sub-domain V^0 , lying in the middle with the width a , encloses the

fixed floating obstacle (see Fig. 2). Here, we considered the parameters of Fig. 1 as $b = 0$ and $c = W$, and Fig. 4 shows the boundary of the floating obstacle in such a case. This curve represents the witted part of the boundary of the floating ship.

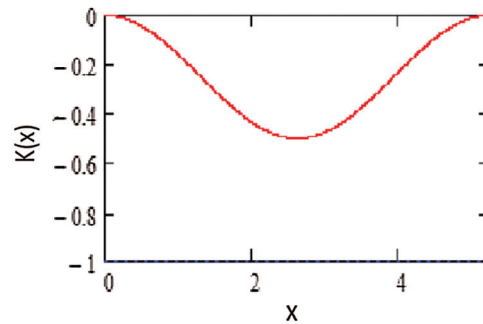


Figure 4: The upper bound of the region V^0

5.1 Reliability of the Method

We find the error $ER_G^{(N,M)}$ for some choices of the numbers M and N in Tab. 1. The numerical values given to the different parameters are taken as $\omega = \sqrt{g/h}$, $H/h = 0.5$ and $W/h = a/h = 5.2373$. The value of $\lambda_0 h$ is 1.1997 and we have taken $k_0 = 1$ which results $a/h = 2k_0\pi/(\lambda_0 h) = 5.2373 = W/h$ as required. The nodes $\{x_n, n = 0, 1, 2, \dots, N\}$ in $0 \leq x \leq a$ are assumed equidistant.

Table 1: The errors $ER_G^{(N,M)}$ for the fixed floating obstacle of Eq. (58)

M	$N = M$	$M + 20$	$M + 40$
30	1.112×10^{-4}	2.117×10^{-6}	6.857×10^{-7}
40	1.484×10^{-5}	5.290×10^{-6}	1.319×10^{-6}
100	5.474×10^{-6}	6.849×10^{-6}	1.725×10^{-6}
150	1.561×10^{-6}	4.717×10^{-7}	2.387×10^{-6}
200	7.199×10^{-7}	8.524×10^{-8}	3.095×10^{-7}
250	3.980×10^{-7}	2.357×10^{-7}	7.360×10^{-8}
260	1.601×10^{-7}	3.118×10^{-7}	3.306×10^{-7}
270	1.533×10^{-7}	2.183×10^{-7}	3.416×10^{-6}
300	2.328×10^{-7}	8.670×10^{-8}	5.652×10^{-6}

Tab. 1 indicates that, the efficiency of the method is in general acceptable and that for $N \geq 100$, the error oscillates between 10^{-8} and 10^{-6} . The values $N = 250$ and $M = 290$ give the best result in the table. For the present application there is an optimum value of $M(M + 1 = 251)$ and hence it is not recommended to increase the number M without limit.

Fig. 5 exhibits $|ER^{(N,M)}(x)|$ along $0 \leq x \leq a$ for the values $M = 250$ and $N = 290$. As shown, this error is localized near the bounds of the fixed floating obstacle at $x = 0$ and at $x = W$.

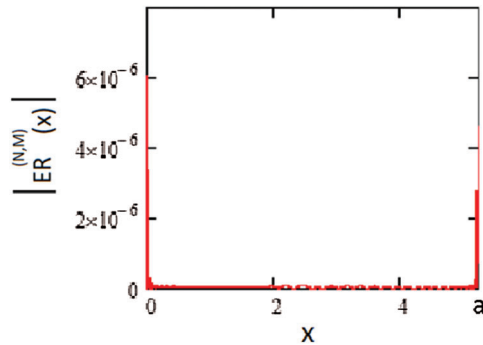


Figure 5: The error $ER^{(N,M)}(x)$ for $M = 250$ and $N = 290$

The conservation of energy relation (42) associated with the error distribution shown on Fig. 5 is $\left| \frac{T_0}{I_0} \right|^2 + \left| \frac{R_0}{I_0} \right|^2 = 1.0002$, with an error of the order of 10^{-4} . while the conservation of mass relation (43) is satisfied identically.

5.2 The System of Streamlines

Streamlines are a family of curves that are instantaneously tangent to the velocity vector of the flow. The stream function $\Psi(x, y)$ assumes constant value on each streamline and the general equation of this family takes the form

$$\Psi(x, y) = const., \tag{62}$$

where different values of the constant on the R.H.S. of Eq. (62), gives different streamlines.

Fig. 6 illustrates the system of streamlines, in the present application, inside the extended region V .

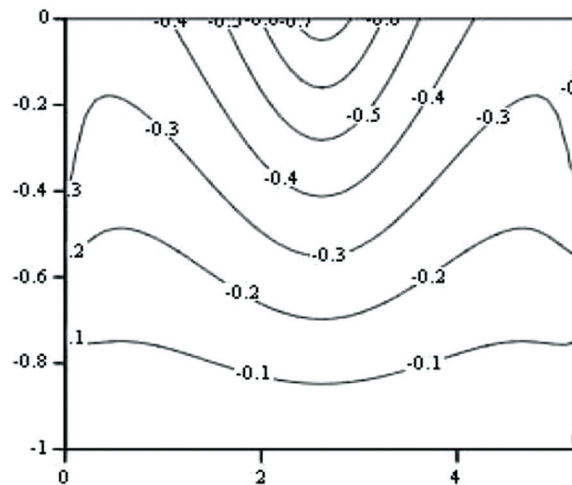


Figure 6: The system of streamlines inside the control region V

Fig. 7 illustrates the system of streamlines inside the control region V^0 . The number assigned to each line refers to the constant value of the function $Re(\Psi^0(x, y)/I_0)$ along this line.

The horizontal bottom of the channel is the lowest streamline ($\Psi^0(x,y) = 0$) and the lower boundary of the fixed floating obstacle is a part of another streamline ($\Psi^0(x,y) = C_0$). For the present application $Re\left(\frac{C_0}{I_0}\right) = -0.336$.

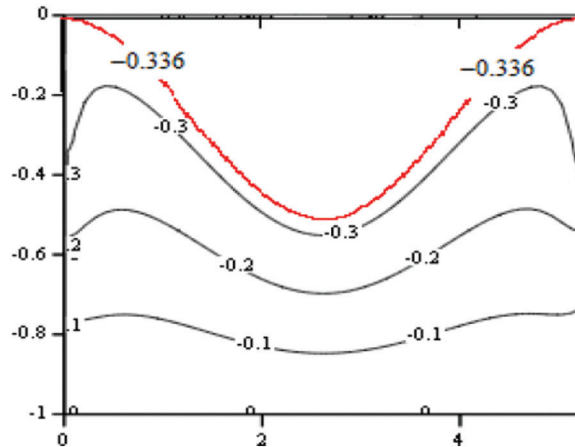


Figure 7: The system of streamlines inside the control region V^0

Fig. 7 shows that the fluid particles are accelerated when approaching the fixed floating obstacle.

5.3 Pressure Applied to the Immersed Part of the Fixed Floating Obstacle

The calculation of the dynamical pressure acting on the witted part of the boundary of the fixed floating obstacle (which simulates the floating ship) has a certain practical interest. Fig. 8 illustrates the real part of the dimensionless dynamical pressure along this boundary. The figure shows that the pressure is greater on the side facing the incident wave direction and decreases till attaining its minimum value on the other side.

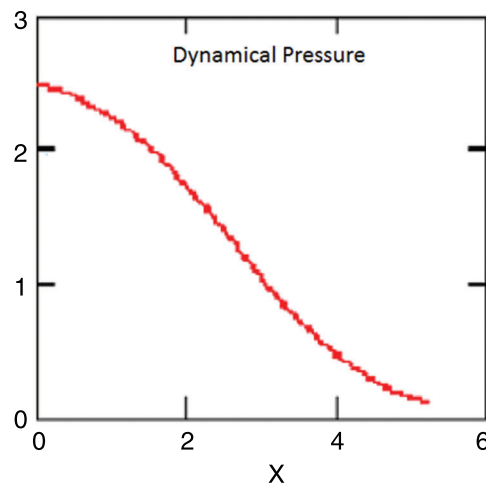


Figure 8: The dynamical pressure acting on the boundary of the fixed floating obstacle

6 Conclusions

The objective of the present work is to study a model, simulating the phenomenon of reflection and transmission of an incident wave on a floating ship in a vast ocean. The obtained results may be used in checking the reliability of other methods proposed for studying the same problem. We satisfy exactly the equations and the conditions of the problem except for the condition on the fixed obstacle's which we satisfy approximately.

The worked applications show that the method is easy to use with reasonable numerical calculations. The accuracy of the method is tested on a particular worked application and the resulting system of streamlines is given and the dynamical pressure acting on the witted part of the surface of the fixed floating obstacle is calculated as well. The limiting case of a floating obstacle having the form of a vertical partially immersed thin barrier needs another procedure for the study and is in progress. This case needs special care.

If the boundary of the floating body contains corner points [25], the solution is singular. This is not physical and comes from the mathematical treatment. To avoid this inconvenient result the corner points should be smoothed to a convenient order.

Funding Statement: The author received no specific funding for this study.

Conflicts of Interest: The author declare that they have no conflicts of interest to report regarding the present study.

References

- [1] W. Thomson, "On stationary waves in flowing water, Part I," *Philosophical Magazine*, vol. 5, pp. 353–357, 1886.
- [2] W. Thomson, "On stationary waves in flowing water, Part II," *Philosophical Magazine*, vol. 5, pp. 445–452, 1887.
- [3] L. Huang, K. Ren, M. Li, Z. Tukovic, P. Cardiff *et al.*, "Fluid-structure interaction of a large ice sheet in waves," *Ocean Engineering*, vol. 182, pp. 102–111, 2019.
- [4] M. Farhat, "Scattering theory of gravity-flexural waves of floating plates water," *Physical Review B*, vol. 101, no. 1, pp. 14307, 2020.
- [5] S. H. Lamb, "Hydrodynamics," *Dover Book on Physics*, Sixth Revised ed., New York, 1994.
- [6] J. V. Wehausen and E. V. Laitone, *Surface waves Handbuch der Physik*, vol. 9. Berlin: Springer, 1966.
- [7] M. S. Abou-Dina and M. A. Helal, "The influence of a submerged obstacle on an incident wave in stratified shallow water," *European Journal of Mechanics - B/Fluids*, vol. 9, pp. 545–564, 1990.
- [8] M. S. Abou-Dina and M. A. Helal, "The effect of a fixed barrier on an incident progressive wave in shallow water," *Nuovo Cimento B*, vol. 107, pp. 331–344, 1992.
- [9] M. S. Abou-Dina and M. A. Helal, "The effect of a fixed submerged obstacle on an incident wave in stratified shallow water (Mathematical Aspects)," *Nuovo Cimento B*, vol. 110, pp. 927–942, 1995.
- [10] J. J. Xie, H. W. Liu and P. Lin, "Analytical solution for long-wave reflection by a rectangular obstacle with two scour trenches," *Journal of Engineering Mechanics*, vol. 137, pp. 919–930, 2011.
- [11] M. S. Abou-Dina, "Nonlinear transient gravity waves due to an initial free surface elevation over a topography," *Journal of Computational and Applied Mathematics*, vol. 130, pp. 173–195, 2001.
- [12] C. Hazard, "On the absence of trapped modes in locally perturbed open waveguides," *IMA Journal of Applied Mathematics*, vol. 80, pp. 1049–1062, 2015.
- [13] J. T. Kirby, "A general wave equation for waves over rippled beds," *Journal of Fluid Mechanics*, vol. 162, pp. 171–186, 1986.
- [14] J. Miles, "On gravity-wave scattering by non-secular changes in depth," *Journal of Fluid Mechanics*, vol. 376, pp. 53–60, 1998.

- [15] J. Miles and P. Chamberlain, "Topographical scattering of gravity waves," *Journal of Fluid Mechanics*, vol. 361, pp. 175–188, 1998.
- [16] P. F. Rhodes-Robinson, "On the forced surface waves due to a partially immersed vertical wavemaker in water of infinite depth," *Quarterly of Applied Mathematics*, vol. 4, pp. 709–719, 1996.
- [17] F. Nelli, L. G. Bennetts, D. M. Skene, J. P. Monty, J. H. Lee *et al.*, "Reflection and transmission of regular water waves by a thin floating plate," *Wave Motion Journal*, vol. 70, pp. 209–221, 2017.
- [18] R. W. Yeung, "Numerical methods in free-surface flows," *Annual Review of Fluid Mechanics*, vol. 14, pp. 395–442, 1982.
- [19] J. A. Kolodziej, "Review of application of boundary collocation methods in mechanics of continuous media," *Mathematics*, vol. 12, pp. 187–231, 1987.
- [20] A. P. Zielinski and I. Herrera, "Trefftz method: Fitting boundary conditions," *International Journal for Numerical Methods in Engineering*, vol. 24, pp. 871–891, 1987.
- [21] A. H. Nayfeh, *Introduction to perturbation techniques*. New York: Interscience Pub., 1981.
- [22] M. S. Abou-Dina and M. A. Helal, "Reduction for the nonlinear problem of fluid waves to a system of integro-differential equations with an oceanographical application," *Journal of Computational and Applied Mathematics*, vol. 95, pp. 65–81, 1998.
- [23] M. S. Abou-Dina and M. A. Helal, "Boundary integral method applied to the transient nonlinear wave propagation in fluid with initial free surface elevation," *Applied Mathematical Modelling*, vol. 24, pp. 535–549, 2000.
- [24] G. Fairweather and A. Karageorghis, "The method of fundamental solutions for elliptic boundary value problems," *Advances in Computational Mathematics*, vol. 9, pp. 69–95, 1998.
- [25] M. S. Abou-Dina and F. M. Hassan, "Approximate determination of the transmission and reflection coefficients for water-wave flow over a topography," *Applied Mathematics and Computation*, vol. 168, pp. 283–304, 2005.
- [26] A. Abbasnia and M. Ghiasi, "Simulation of irregular waves over submerged obstacle on a NURBS potential numerical wave tank," *Latin American Journal of Solids and Structures*, vol. 11, pp. 2308–2332, 2014.
- [27] M. S. Abou-Dina and A. F. Ghaleb, "Multiple wave scattering by submerged obstacles in an infinite channel of finite depth I. Streamlines," *European Journal of Mechanics - B/Fluids*, vol. 59, pp. 37–51, 2016.
- [28] L. G. Bennetts and T. D. Williams, "Water wave transmission by an array of floating discs," *Proceedings of the Royal Society of London: Series A*, vol. 471, pp. 20140698, 2015.
- [29] W. W. Ding, Z. J. Zou, J. P. Wu and B. G. Huang, "Investigation of surface piercing fixed structures with different shapes for Bragg reflection of water waves," *International Journal of Naval Architecture and Ocean Engineering*, vol. 11, pp. 819–827, 2019.
- [30] N. Drimer, Y. Agnon and M. Stiassnie, "A simplified analytical model for a floating breakwater in water of finite depth," *Applied Ocean Research*, vol. 14, pp. 33–41, 1992.
- [31] N. Kuznetsov and O. Motygin, "On the coupled time-harmonic motion of deep water and a freely floating body: Trapped modes and uniqueness theorems," *Journal of Fluid Mechanics*, vol. 703, pp. 142–162, 2012.
- [32] B. N. Mandal, "Water wave scattering by bottom undulations in the presence of a thin partially immersed barrier," *Applied Ocean Research*, vol. 28, pp. 113–119, 2006.
- [33] P. A. Martin, "Multiple scattering, interaction of time-harmonic waves with N obstacles. bridge University Press, Corrections, and addition, 2006.
- [34] F. Montiel, L. G. Bennetts, V. A. Squire, F. Bonnefoy and P. Ferrant, "Hydroelastic response of floating elastic disks to regular waves. Part 2: Modal analysis," *Journal of Fluid Mechanics*, vol. 723, pp. 604–628, 2013.
- [35] W. Peng, K. H. Lee, S. H. Shin and N. Mizutani, "Numerical simulation of interaction between water wave and inclined-moored submerged floating breakwaters," *Coastal Engineering*, vol. 82, pp. 76–87, 2013.

- [36] R. Shih, C. Chou and J. Yim, "Numerical estimation of wave reflection coefficients for irregular waves over submerged obstacles," *International Journal of Offshore and Polar Engineering*, vol. 246, pp. 19–24, 2005.
- [37] P. J. Cobelli, V. Pagneux, A. Maurel and P. Petitjeans, "Experimental study on water-wave trapped modes," *Journal of Fluid Mechanics*, vol. 666, pp. 445–476, 2011.
- [38] A. S. Koram and O. S. Rageh, "Effect of under connected plates on the Hydrodynamic efficiency of the floating breakwater," *China Ocean Engineering*, vol. 28, pp. 349–362, 2013.
- [39] O. S. Ragih, K. S. El-Alfy, M. T. Shamaa and R. M. Diad, *An Experimental Study of Spherical Floating Bodies Under Waves*. Egypt: IWTC10, pp. 357–375, 2006.
- [40] D. M. Skene, L. G. Bennetts, M. H. Meylan and A. Toffoli, "Modelling water wave over wash of a thin floating plate," *Journal of Fluid Mechanics*, vol. 777, pp. 1–13, 2015.
- [41] Y. Yu, Z. Guo and Q. Ma, "Transmission of water waves under multiple vertical thin plates," *Water*, vol. 10, pp. 517, 2018.
- [42] C. J. Tranter, *Integral Transforms in Mathematical Physics*. 3rd ed., London: Methuen Co. Ltd., 1966.